

# A Novel Anaerobic Electrochemical Membrane Bioreactor (AnEMBR) with Conductive Hollow-fiber Membrane for Treatment of Low-Organic Strength Solutions

Krishna P. Katuri,<sup>†,||</sup> Craig M. Werner,<sup>†,||</sup> Rodrigo J. Jimenez-Sandoval,<sup>†</sup> Wei Chen,<sup>‡</sup> Sungil Jeon,<sup>‡</sup> Bruce E. Logan,<sup>§</sup> Zhiping Lai,<sup>‡</sup> Gary L. Amy,<sup>†</sup> and Pascal E. Saikaly<sup>\*,†</sup>

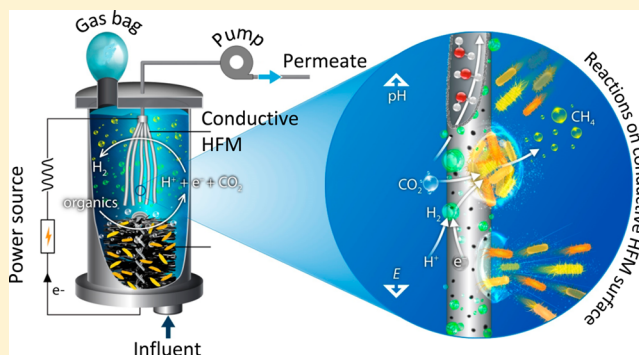
<sup>†</sup>King Abdullah University of Science and Technology, Biological and Environmental Sciences and Engineering Division, Water Desalination and Reuse Center, Thuwal 23955–6900, Saudi Arabia

<sup>‡</sup>King Abdullah University of Science and Technology, Advanced Membranes and Porous Materials Research Center, Thuwal 23955–6900, Kingdom of Saudi Arabia

<sup>§</sup>Department of Civil and Environmental Engineering, Pennsylvania State University, University Park, Pennsylvania 16802, United States

## Supporting Information

**ABSTRACT:** A new anaerobic treatment system that combined a microbial electrolysis cell (MEC) with membrane filtration using electrically conductive, porous, nickel-based hollow-fiber membranes (Ni-HFMs) was developed to treat low organic strength solution and recover energy in the form of biogas. This new system is called an anaerobic electrochemical membrane bioreactor (AnEMBR). The Ni-HFM served the dual function as the cathode for hydrogen evolution reaction (HER) and the membrane for filtration of the effluent. The AnEMBR system was operated for 70 days with synthetic acetate solution having a chemical oxygen demand (COD) of 320 mg/L. Removal of COD was >95% at all applied voltages tested. Up to 71% of the substrate energy was recovered at an applied voltage of 0.7 V as methane rich biogas (83% CH<sub>4</sub>; < 1% H<sub>2</sub>) due to biological conversion of the hydrogen evolved at the cathode to methane. A combination of factors (hydrogen bubble formation, low cathode potential and localized high pH at the cathode surface) contributed to reduced membrane fouling in the AnEMBR compared to the control reactor (open circuit voltage). The net energy required to operate the AnEMBR system at an applied voltage of 0.7 V was significantly less (0.27 kWh/m<sup>3</sup>) than that typically needed for wastewater treatment using aerobic membrane bioreactors (1–2 kWh/m<sup>3</sup>).



## INTRODUCTION

Water and energy resources are interdependent; a relationship commonly referred to as the water-energy nexus.<sup>1</sup> As the global demand for freshwater continues to place significant pressure on available water resources, domestic wastewater reclamation and reuse represents a viable water resource. However, domestic wastewater treatment processes based on conventional activated sludge are energy intensive and consume on the order of 0.6 kWh/m<sup>3</sup> of wastewater treated, 50% of which is used for aeration.<sup>2</sup> As domestic wastewater is estimated to contain ~2 kWh/m<sup>3</sup> of energy in the form of organic substrate,<sup>3</sup> an opportunity exists to offset energy consumption for domestic wastewater treatment through recovery of the inherent energy and move toward energy neutral or energy positive wastewater treatment.

Processes based on bioelectrochemical systems (BES) such as microbial fuel cells (MFCs) and microbial electrolysis cells (MECs) hold promise for the treatment of wastewater with

concomitant energy recovery. Microbial fuel cells use bacteria capable of transferring electrons exogenously to convert soluble organic matter present in the wastewater directly into electricity. MECs are similar to MFCs but can generate hydrogen from biodegradable organic matter.<sup>4–6</sup> By excluding oxygen from the system and applying an additional voltage to the circuit, hydrogen is evolved at the surface of the cathode electrode.<sup>6</sup> Bioelectrochemical systems are effective at treating low strength wastewaters,<sup>7</sup> such as domestic wastewater,<sup>8,9</sup> and they can also be operated at temperatures below 20 °C.<sup>10</sup> However, these systems alone are not able to produce the high quality effluent that is needed for water reuse applications.

Received: April 8, 2014

Revised: October 11, 2014

Accepted: October 13, 2014

Published: October 13, 2014

To improve the effluent quality from MFCs, a number of studies have reported systems that integrate MFCs with membrane bioreactors (MBRs).<sup>11–18</sup> In most cases these systems were not truly integrated as the two processes were separated in either a single-stage<sup>11–17</sup> or two-stage system.<sup>18</sup> Recently, Malaeb et al. reported a truly integrated proof-of-concept hybrid MFC-MBR system that incorporated a conductive, flat-sheet ultrafiltration membrane biocathode within a MFC.<sup>19</sup> The conductive porous flat sheet cathode provided the dual function as the cathode for oxygen reduction reaction and the membrane for filtration of the effluent. However, a disadvantage of using a conductive porous flat sheet cathode is their low specific surface area (i.e., cathode surface area per reactor volume). Increasing the packing density of the cathode is a critical aspect of the design of BES for practical applications for wastewater treatment. Also, the current density in MFCs has to be increased considerably (i.e., by lowering the internal resistance) for commercial applications, whereas MECs have already been used in commercial applications<sup>20</sup> as their current density can be increased by increasing the applied voltage.<sup>21</sup>

Studies on the integration of MECs with MBRs have not been reported previously. Here we proposed a novel system that integrates the operating principles of a MEC with anaerobic filtration using electrically conductive, porous nickel-based hollow fiber membranes (Ni-HFM) to recover the energy from a low organic strength solution (300 mg/L of COD) directly as biogas and reclaim the treated water in what is called an anaerobic electrochemical membrane bioreactor (AnEMBR). The advantage of using a conductive porous Ni-HFM as cathode material is that it allows for a truly integrated hybrid MEC-MBR system with the dual benefit of energy and water recovery in a single stage. Also, the novel cathode design overcomes the challenge to maximize the electrode surface area to reactor volume ratio by increasing the packing density of the cathode, which is required for large-scale applications of MECs. However, a major challenge of integrating MECs with membrane filtration processes is membrane fouling, which is a major drawback of all MBRs. Membrane fouling contributes significantly to both capital and operation costs that arise from the need to clean or replace membranes. Therefore, to become an attractive option for the treatment of low organic strength solutions, the energetic efficiency and fouling of the novel AnEMBR system are important measures of evaluation.

Applied voltage is one of the most important parameters affecting the performance of MECs. The applied voltage can affect the energy balance and rate of hydrogen evolution.<sup>21</sup> Increasing the applied voltage increases the rate of hydrogen evolution,<sup>21</sup> and it is expected that membrane fouling could be minimized due to the scouring effect of the increased rate of gas bubble formation at the surface of the membrane. Therefore, the objective of this study was to evaluate the effect of different applied voltages (0.5, 0.7, and 0.9 V) on the performance of the AnEMBR system in terms of energy recovery and membrane fouling. Also, the performance of the system was quantified in terms of Coulombic efficiency (CE), current density, biogas composition, volumetric gas production rate and permeate quality.

## MATERIALS AND METHODS

**Preparation of Conductive Ni-HFM.** The cathode was configured using a Ni-HFM with an average pore size of 1  $\mu\text{m}$  (Figures 1A–C). Each fiber was 10 cm long with an outer

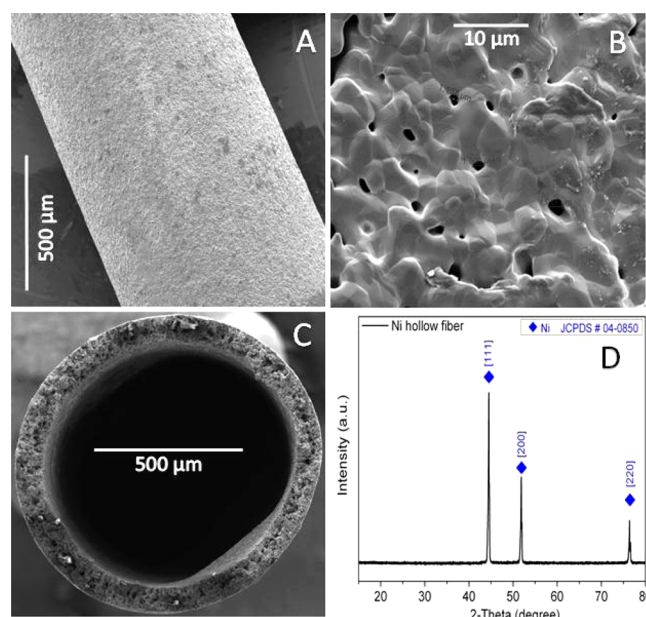


**Figure 1.** Scanning electron micrographs of a virgin nickel hollow fiber membrane showing the outer surface of the membrane (A), a close-up of the outer surface with pores visible (B) and a cross section of the fiber (C). The XRD pattern of the Ni-HFM (D).

diameter of 0.09 cm giving a surface area of 2.8  $\text{cm}^2$  per fiber, for a total surface area of 4  $\text{m}^2/\text{m}^3$ . Five fibers were connected together at one end using conductive silver epoxy. The Ni-HFM were fabricated using a combined phase-inversion/sintering method.<sup>22</sup> Briefly, nickel powders, 1-methyl-2-pyrrolidinone (NMP, HPLC grade, 99.5%, Alfa Aesar), Polyether Sulfone (PES, Ultrason E6020P, BASF) and Polyvinylpyrrolidone (PVP, Alfa Aesar) were mixed and well dispersed by ball milling for 18 h, followed by degassing under vacuum for 24 h. After that, the suspension was extruded through a spinneret using water as the inner and outer coagulant. The blackbody of the hollow fiber was dried at room temperature and then sintered at 560  $^{\circ}\text{C}$  for 6 h to remove organic compounds in air flow of 500  $\text{mL}/\text{min}$ . After cooling to room temperature, the fiber was reduced from the metal oxide state to the metal state at 810  $^{\circ}\text{C}$  for 6 h in pure hydrogen gas at a flow rate of 500  $\text{mL}/\text{min}$ . Characterization by X-ray diffraction (XRD) revealed three diffraction peaks, corresponding to Ni [111], [200], [220] planes (JCPDS No. 04-0850) of face centered cubic (FCC) crystal structure, respectively (Figure 1 D).

**Reactor Construction and Operation.** The tubular AnEMBR (23 cm length, 4.5 cm internal diameter) was constructed from plexiglass and had a working volume of 350 mL. A vertical cylinder (0.5 cm wall thickness) was sandwiched between the plexiglass central-grooved end plates (2 cm thick), sealed with a rubber “O ring” gasket, and bolted together. Ports for feed inlet and anode-current collector were made at the bottom end plate. Additional ports were positioned on the top end plate of the reactor for gas and permeate collection and for cathode current collector. Also, an outlet for effluent recirculation and head space gas sampling port were provided on top lateral sides of the reactor. The anode was a graphite fiber brush (10 cm  $\times$  5 cm, PANEX 33 160 K, ZOLTEK) containing a titanium core that was heat treated at 450  $^{\circ}\text{C}$  for 15 min. The anode was positioned vertically at the bottom of

the reactor. The cathode was positioned vertically at the top of the reactor with the ends of the fibers positioned approximately 2 cm from top of the anode. One end of a silicone tube was placed over the top of the cathode and the other connected to a peristaltic pump for filtration. Care was taken to ensure all connections were well sealed with nonconductive epoxy. A schematic representation of the reactor is presented in Figure 2.

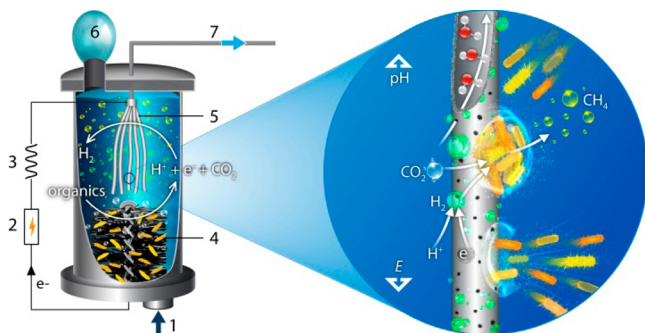


**Figure 2.** Schematic representation of the AnEMBR (1. feed, 2. power supply, 3. 10  $\Omega$  external resistor, 4. anode, 5. Ni-HFM cathode, 6. gas bag, 7. permeate). The dual purpose cathode fiber contain pores that enable water transport as shown in the magnified section of the figure.

The reactor was operated in MEC mode, and fed with acetate (0.32 g/L as COD) in a buffered medium containing (g/L):  $\text{NH}_4\text{Cl}$ , 1.5;  $\text{Na}_2\text{HPO}_4$ , 0.6;  $\text{KCl}$ , 0.1 and 2.5,  $\text{Na}_2\text{HCO}_3$ ; and trace minerals and vitamin solutions.<sup>23</sup> The final conductivity of the solution was 2.9 mS/cm with a pH of 6.9. The reactor was inoculated with anaerobic digester sludge (10% v/v, Manfouha Wastewater Treatment Plant, Riyadh, KSA). For the first four batches, the feed was supplemented with inoculum and subsequent cycles contained only medium without any inoculum. An applied voltage of 0.7 V was used to acclimate the reactor under fed-batch operation for two months prior to obtaining experimental results. An external power source (3645A; Circuit Specialists, Inc., AZ) was used to apply voltage to the circuit, and a data logger (ADC 24, PicoLog, UK) was connected to monitor the voltage across an external resistor ( $R_{\text{ex}} = 10 \Omega$ ) to calculate current. After completion of the acclimation period the Ni-HFM was replaced with virgin Ni-HFM and the reactor was operated for an additional 70 days at room temperature (25  $^\circ\text{C}$ ). Three applied voltages (0.5, 0.7, and 0.9 V) were tested during this period. At the end of each experimental batch cycle, when the voltage dropped to 10 mV, the treated medium was filtered through the cathode filters using a peristaltic pump (Masterflex L/S, Cole-Parmer, Vernon Hills, IL.) at a permeate flux of 6.9 L/m<sup>2</sup>/h (LMH). The transmembrane pressure (TMP) of the membrane filters was measured by means of a pressure transducer (68075–32, Cole-Parmer Instrument Company) attached to the filtrate line, and recorded using a data acquisition device (LabJack U6, LabJack Corporation, Lakewood, CO) connected to a computer. A new cycle was started after fresh medium was pumped into the reactor.

A control reactor (open circuit voltage) was constructed similarly to the AnEMBR system and was operated in parallel under the same conditions in order to compare the fouling propensity of the Ni-HFM in terms of TMP.

**Energy Recovery Calculations.**<sup>24</sup> The moles ( $n$ ) of gas produced from the measured gas volume were calculated using

$$n(\text{mol}) = \frac{v}{TR} \quad (1)$$

where  $v$  is the volume of gas (L),  $T$  is the temperature (298 K) and  $R$  is the gas constant (0.08206 L-atm/K-mol. The energy content of the biogas produced is

$$W_{\text{Gas}}(\text{kJ}) = n_{\text{H}_2}\Delta H_{\text{H}_2} + n_{\text{CH}_4}\Delta H_{\text{CH}_4} \quad (2)$$

where  $n_{\text{H}_2}$  is the number of moles of hydrogen produced,  $\Delta H_{\text{H}_2} = 285.83$  kJ/mol is the energy content of hydrogen based on the heat of combustion (upper heating value),  $n_{\text{CH}_4}$  is the number of moles of methane produced and  $\Delta H_{\text{CH}_4} = 891$  kJ/mol is the energy content of methane.  $W_{\text{Gas}}$  was converted to kWh using a conversion factor of 0.000278 (1 kWh = 3600 kJ) and normalizing this power consumption to the reactor volume (m<sup>3</sup>).

The moles of hydrogen and methane ( $n_{\text{CE}}$ ) that can be recovered based on the measured current were calculated using

$$n_{\text{CE}}(\text{H}_2) = \frac{\int_{t=0}^t I dt}{2F} \quad (3)$$

$$n_{\text{CE}}(\text{CH}_4) = \frac{\int_{t=0}^t I dt}{8F} \quad (4)$$

where  $I = V/R_{\text{ex}}$  is the current (A) calculated from the voltage across the resistor (10  $\Omega$ ), 2 is the moles of electrons per mole of hydrogen, 8 is the moles of electrons per mole of methane (assuming 4 mol hydrogen to produce 1 mol methane),  $F = 96485$  C/mol  $e^-$  is Faraday's constant, and  $dt$  (s) is the time interval (20 min) over which data were collected. The moles of hydrogen and methane actually recovered relative to that possible based on the measured current is the cathodic recovery,  $r_{\text{Cat}}$  calculated using

$$r_{\text{Cat}}(\text{H}_2) = \frac{n_{\text{H}_2}}{n_{\text{CE}}} \quad (5)$$

$$r_{\text{Cat}}(\text{CH}_4) = \frac{n_{\text{CH}_4}}{n_{\text{CE}}} \quad (6)$$

where  $n_{\text{H}_2}$  and  $n_{\text{CH}_4}$  are the number of moles of hydrogen and methane recovered during a batch cycle.

**Energy Consumption.** The energy consumed for recirculation and filtration was calculated using the pump power requirement equation,<sup>25</sup> as

$$P(\text{kW}) = \frac{Q_1\gamma E_1}{1000} + \frac{Q_2\gamma E_2}{1000} \quad (7)$$

where  $P$  is the power requirement (kW),  $Q_1$  equals the reactor recycle rate of 0.02 L/min ( $3.33 \times 10^{-7}$  m<sup>3</sup>/s),  $\gamma$  is 9800 N/m<sup>3</sup>, and  $E_1$  is the measured hydraulic pressure head loss through the system of 0.05 m,  $Q_2$  is the permeate flow rate of 0.0096 L/h ( $2.67 \times 10^{-9}$  m<sup>3</sup>/s) and  $E_2$  is the head loss due to TMP (m). Dividing the overall power requirement (kW) by the permeate flow rate ( $9.6 \times 10^{-6}$  m<sup>3</sup>/h) yields the pumping energy requirement of the system in kWh/m<sup>3</sup>.

The amount of energy added to the system by the power source, adjusted for losses across the resistor ( $W_E$ ) is given by

$$W_E(\text{kJ}) = \sum_{i=1}^n (IE_{\text{ps}}\Delta t - I^2R_{\text{ex}}\Delta t) \quad (8)$$



Table 1. Performance of the AnEMBR at Different Applied Voltages

$E_{ap}$ (V)	CE <sup>42</sup> (%)	H <sub>2</sub> rate (m <sup>3</sup> /m <sup>3</sup> /d)	CH <sub>4</sub> rate (m <sup>3</sup> /m <sup>3</sup> /d)	$r_{Cat}$ % (H <sub>2</sub> )	$r_{Cat}$ % (CH <sub>4</sub> )
0.5 <sup>a</sup>	53 ± 11.4	0.001 ± 0.001	0.011 ± 0.002	1.1 ± 1.5	72.2 ± 21.8
0.7 <sup>b</sup>	66	0.025	0.016	15.8	41.3
0.7 <sup>c</sup>	81 ± 8.8	0.000 ± 0.000	0.028 ± 0.006	0.1 ± 0.2	86.5 ± 15.6
0.9 <sup>d</sup>	57	0.20	0.01	115.9	29.1
0.9 <sup>e</sup>	65 ± 5.5	0.05 ± 0.025	0.03 ± 0.005	22.3 ± 10.7	50.1 ± 9.7

<sup>a</sup>Average of two reproducible cycles of operation at 0.5 V. <sup>b</sup>First cycle of operation at 0.7 V. <sup>c</sup>Average of three reproducible cycles of operation at 0.7 V, days 14–21. <sup>d</sup>First cycle of operation at 0.9 V. <sup>e</sup>Average of final three reproducible cycles of operation at 0.9 V.

where  $E_{ps}$  (V) is the applied voltage using the power source,  $\Delta t$  (s) is the time increment for  $n$  data points measured during a batch cycle, and  $R_{ex} = 10 \Omega$  is the external resistor in the circuit.  $W_E$  is converted to kWh using a conversion factor of 0.000278 and normalizing this power consumption by volume (m<sup>3</sup>).

**Energy Efficiency Calculations.**<sup>24</sup> The energy efficiency relative to the electrical input ( $\eta_E$ ) is the ratio of the energy content of the biogas produced to the input electrical energy required, or

$$\eta_E = \frac{W_{Gas}}{W_E} \quad (9)$$

The efficiency relative to the added substrate ( $\eta_S$ ) is given by

$$\eta_S = \frac{W_{Gas}}{W_S} \quad (10)$$

where  $W_S$  is the amount of energy added by the substrate given by

$$W_S(\text{kJ}) = n_S \Delta H_S \quad (11)$$

where  $\Delta H_S = 870 = 870.28 \text{ kJ/mol}$  is the heat of combustion of the substrate (acetate), and  $n_S$  is the number of moles of substrate consumed.

**Analyses.** Total suspended solids (TSS) were measured using standard methods.<sup>26</sup> Samples for acetate analysis were filtered through 0.20  $\mu\text{m}$  pore diameter syringe filters prior to analysis to remove any particulate matter. Acetate concentrations were measured with an Aminex HPX-87H Ion Exclusion Column (Bio-Rad Laboratories, Hercules, CA) using 5 mM sulfuric acid solution as mobile phase at a flow rate of 0.55 mL/min. The HPLC unit was an Accela HPLC system (Thermo Scientific) fitted with a photodiode array (PDA) detector. Peaks were detected at 210 nm. Soluble chemical oxygen demand (SCOD) was analyzed using a spectrophotometer (HACH DR/2010, HACH Co., Loveland, CO).

Biogas was collected in a gas bag connected to the top of the reactor. At the end of each batch cycle, the gas composition in the reactor headspace and gas bag was analyzed using a gas chromatograph (model 310, SRI Instruments) according to methods described previously.<sup>6</sup>

The biofilms on the Ni-HFM membranes were examined using a scanning electron microscope (SEM). Prior to SEM imaging, new and biofilm covered membranes were dehydrated in a series of graded alcohol solutions and oven-dried (2 h at 30 °C). The samples were mounted either flat onto an aluminum stub using thin aluminum tape or vertically inside a machined slot aluminum stub using carbon paste. After sputter-coating the samples with gold palladium for 30 s at 25 mA current in an argon atmosphere, SEM imaging (Quanta 200D, FEI, The

Netherlands) was performed using an accelerating voltage of 25 kV and working distance of 10 mm.

## RESULTS AND DISCUSSION

**Performance of the AnEMBR at Different Applied Voltages.** As described in the Materials and Methods section, the reactor was dismantled after two months of stable anodic biofilm formation at 0.7 V and the conductive Ni-HFMs were replaced with fresh fibers. The system was initially operated at 0.7 V with these new fibers that were in place for the remainder of the experiment. The extended exposure of the anodic biofilm to air and biofilm disturbance during the replacement process of HFM affected the electrogenesis activity for the first cycle of operation (0.7<sup>b</sup>, Table 1). However, in the successive batch operations, anodic activity was recovered with consistent reproducibility in CE between the fed-batch cycles. When the applied voltage was changed from 0.5 to 0.9 V (a significant increase in voltage), the imposed individual electrode potentials also changed and these immediate changes in the electrode potentials influenced the bacterial physiology, and thus influenced the CE in the first cycle (0.9<sup>d</sup>, Table 1). However, in the successive fed-batch cycles of operations the CE was improved with consistent reproducibility. These results demonstrate the robustness of the AnEMBR system when operating conditions are changed where reproducible performance is attained after one cycle of operation. Also, these systems are highly reproducible once the anodic biomass is established. For example, a similar current was produced when the AnEMBR was switched back to 0.7 V (38th day) following 10 days of operation under open circuit voltage (Figure 3). This observation provided evidence for a well-established and stable anodic biofilm with performance that was representative of a typical BES anodic biofilm. Further evidence of reproducibility is provided in the Supporting Information (SI) where a duplicate AnEMBR performed similarly in terms of current density and CE (SI Table S2) with the evolution of the same anodic communities in the duplicate reactor.

At an applied voltage of 0.7 V the AnEMBR produced an average volumetric current density of 11.1 A/m<sup>3</sup> or 2.7 A/m<sup>2</sup> based on cathode surface area (4.1 m<sup>2</sup>/m<sup>3</sup>) (Figure 3) with an average CE of 81% (Table 1). After two months of acclimation at an applied voltage of 0.7 V, the system produced a biogas composed predominantly of hydrogen when virgin Ni-HFM was first placed into the system (day 0, cycle 1) at a maximum rate of 0.025 m<sup>3</sup>H<sub>2</sub>/m<sup>3</sup>/d (Table 1). The biogas composition shifted to >80% methane gas for the following batch cycles with hydrogen gas concentrations contributing <1% of the total gas composition (Figure 3). The extended acclimation period likely provided a suitable amount of time for hydrogenotrophic methanogens to establish a sufficiently high abundance within the reactor to colonize the membrane surface, providing an explanation for the rapid onset of methane production.

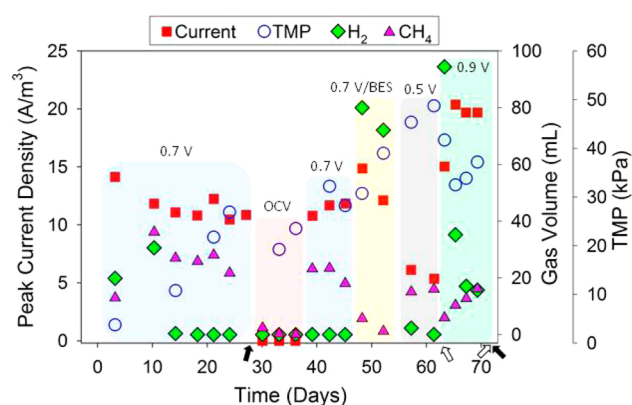


**Figure 3.** Peak current density, volumes of gas produced and TMP of the AnEMBR measured over the course of the experiment. The data for the second cycle at 0.7 V has been omitted due to anomalous cycle duration, likely a result of an error in media preparation. OCV refers to operation under open circuit voltage whereby the electrodes are disconnected and no current flows. BES refers to 2-bromoethanesulfonate, a compound that selectively inhibits methyl-CoM reductase, the terminal enzyme for methane production. Filled arrows represent the time points at which the biofouled Ni-HFM were sampled for qPCR analysis. Unfilled arrows show the points when the biofouled Ni-HFM were sampled for SEM analysis.

The measured methane gas represented a cathodic methane recovery ( $r_{\text{Cat}}$ ) of more than 80% when operated at 0.7 V (Table 1). This means that it was possible to recover a large fraction of the theoretical maximum number of moles of methane possible based on the measured current. Maximum methane production averaged  $0.028 \pm 0.006 \text{ m}^3/\text{m}^3/\text{d}$  at an applied voltage of 0.7 V (Table 1).

Although the generation of methane is documented in single-chamber MEC systems,<sup>6,24,27,28</sup> the main route of methane generation and the archaeal methanogenic community composition were rarely studied. The methane produced in the AnEMBR system was mainly via hydrogenotrophic methanogenesis. This conclusion was based on (i) the absence of methane gas when the system was operated in open circuit mode (i.e., no HER) for three cycles (Figure 3, days 30–38); and (ii) quantitative PCR (qPCR) analysis (detailed information in the SI), which revealed the dominance of the hydrogenotrophic methanogen, *Methanobacteriales* (99.8%), on the cathode with low abundance of *Methanosarcinacea* (0.2%), a mixotrophic methanogen, while acetoclastic methanogens were hardly detected in solution or on the electrodes. and (iii) the addition of 50 mM of 2-bromoethanesulfonate, a known inhibitor of methanogenesis, resulted in a significant drop in methane yields and increase in hydrogen yields (Figure 3 days 49–53). The localized  $\text{H}_2$  availability and high pH at the cathode surface (due to proton consumption of the HER)<sup>29</sup> seemed to favor the growth of *Methanobacteriales*. Some species of *Methanobacteriales* are known to be alkaliphilic, thriving at pH values between 8.1 and 9.1.<sup>30</sup> Observations based on qPCR analysis suggest that *Methanobacteriales* were enriched on the Ni-HFM over the course of AnEMBR operation where the ratio of *Methanobacteriales* to bacteria increased significantly from 0.06 (day 27) to 0.47 (day 71).

At all applied voltages, the methane gas measured did not exceed the maximum that could be achieved based on stoichiometric conversion of current into methane (8 mol of electrons per mol of methane) (SI Figure S1). Comparing the

theoretical hydrogen and methane production rates based on the stoichiometric maximum that could be achieved from the measured current with the actual measured hydrogen and methane gas production rates (detailed analysis in the SI) further supports that hydrogenotrophic methanogenesis was the dominant mechanism of methane generation (SI Figure S1).

The addition of 50 mM 2-bromoethanesulfonate at an applied voltage of 0.7 V inhibited the conversion of hydrogen to methane resulting in significantly higher yields of hydrogen gas as well as an increase in CE to 80% (Figure 3 days 49–53). The measured hydrogen gas represented a cathodic hydrogen recovery ( $r_{\text{Cat}}$ ) of 55% in the presence of 50 mM 2-bromoethanesulfonate and was produced at a considerably higher rate ( $0.091 \text{ m}^3\text{H}_2/\text{m}^3/\text{d}$ ) (Figure 3). Methane gas was still present in the produced biogas, but at much lower concentrations (7%), which showed that methanogens were not completely inhibited and some hydrogen was converted to methane (Figure 3). The hydrogen production rate ( $0.091 \text{ m}^3\text{H}_2/\text{m}^3/\text{d}$ ) measured in the presence of 2-bromoethanesulfonate was lower than those reported for other MEC configurations (SI Table S3). It should be noted that the AnEMBR system reported here was designed only for “proof of concept” and thus was not optimized for performance. Further optimization is required to make a fair comparison with reported bench mark MEC configurations such as those operated with small volumes, smaller electrode distance, high specific area and expensive and effective Pt catalysts (SI Table S3). Nickel was used as a cathode material in this study because it (1) is the most investigated non-noble metal catalyst in MEC studies;<sup>31–33</sup> (2) has a lower hydrogen evolution reaction (HER) overpotential compared to most other non-noble metal catalysts;<sup>31</sup> (3) is more stable under alkaline conditions compared to most other non-noble metal catalysts;<sup>34</sup> the pH at the cathode surface is likely to be alkaline due to the consumption of protons;<sup>31</sup> and (4) most importantly, it has a lower cost compared to Pt catalysts. The cost of cathode material is an important aspect to consider in the development of bioelectrochemical technologies. SI Table S4 shows the cost of the Ni-HFM cathode ( $14 \text{ cm}^2$ ) compared with platinum catalyzed cathode ( $14 \text{ cm}^2$ ) commonly used in BES research.<sup>35</sup> This comparison is based only on the cost of materials from suppliers. The cost analysis shows that a platinum catalyzed cathode of the same surface area is nearly 70 times more expensive than the Ni-HFM cathode. More than half of the cost of the platinum catalyzed cathode is contributed by the platinum catalyst. The catalyst alone is 35 times the cost of the Ni-HFM cathode. Importantly, the idea of the conductive porous Ni-HFM cathode is not limited to nickel but lends itself to other low cost cathode materials and for further improvement and optimization, to reduce fabrication costs even further.

By reducing the applied voltage to 0.5 V, both the current and biogas production decreased (Figure 3, days 58–62). The rate of biogas production was reduced by more than half to  $0.012 \pm 0.001 \text{ m}^3/\text{m}^3/\text{d}$  and was composed of  $93 \pm 6\%$  methane (Figure 3) due to a longer cycle duration (5 days). It is known that increasing the applied voltage increases the current density resulting in a faster COD removal rate,<sup>21</sup> and hence a shorter cycle time is required to remove COD. The extended batch duration due to lower COD removal rates at lower applied voltages (5 days and 3 days at an applied voltage of 0.5 and 0.7 V) allowed for complete conversion of hydrogen ( $r_{\text{Cat}} \% (\text{H}_2) < 1\%$ ) that had accumulated in the reactor



headspace to methane. In the case of an applied voltage of 0.9 V (cycle duration of 1 day), the rate of hydrogen evolution was faster than its consumption by methanogens for methane. Collectively, these resulted in higher  $r_{\text{Cat}}$  % ( $\text{CH}_4$ ) at lower applied voltages (0.5 and 0.7 V) compared to high applied voltage of 0.9 V (Table 1).

Hydrogen production rates and recoveries can be enhanced in MECs by increasing the applied voltage.<sup>6,21</sup> By applying 0.9 V to the AnEMBR, the current density increased to  $15 \text{ A/m}^2$  ( $3.7 \text{ A/m}^2$ ) in the first cycle of operation and the maximum rate of hydrogen production increased to  $0.20 \text{ m}^3\text{H}_2/\text{m}^3/\text{d}$  (Figure 3 and Table 1). These production rates and recoveries of hydrogen were not sustained though and the methane content of the biogas increased over subsequent cycles (Figure 3). This suggests that methanogens adapted to the increased rate of hydrogen production.

Reporting results of the initial cycle is useful for studying the importance of cathodic corrosion, which may be more noticeable during the initial cycle of operation.<sup>36</sup> In this study values corresponding to the first cycle and the average of reproducible cycles were reported to document the performance of the AnEMBR at 0.7 and 0.9 V (Table 1). The first cycle following an increase of the applied voltage from 0.5 to 0.9 V (0.9<sup>d</sup>, Table 1) showed a cathodic Coulombic recovery in excess (>100%) of that possible from measured current generation suggesting that cathodic corrosion<sup>36</sup> occurred as a result of the sudden change toward a more negative cathode electrode potential. However, this corrosion effect was less important over successive fed-batch operations (cathodic Coulombic recovery <100%) due to the high stability of nickel under alkaline conditions,<sup>31,34</sup> and these observations were consistent with the literature that report stable performance of nickel as cathode material compared to alternative nonprecious metals as cathode materials.<sup>36</sup>

**Membrane Fouling.** The control reactor operated under open circuit voltage fouled faster than the AnEMBR. The TMP of the control reactor reached 54 kPa after 34 days of operation whereas the AnEMBR operated for twice as long before a maximum TMP of  $\sim 50 \text{ kPa}$  (Figure S2) was measured. Since both reactors (i.e., AnEMBR and control reactor) had the same configuration and membrane material, and were operated under the same conditions (i.e., cycle time, organic loading rate, temperature, etc.), it can be concluded that the AnEMBR provided an advantage of fouling limitation over the control reactor.

Membrane fouling is an inevitable phenomenon in aerobic and anaerobic MBRs and it is more problematic under anaerobic than aerobic conditions.<sup>17</sup> Gas sparging is the most widely used method for membrane fouling control in anaerobic MBRs. However, this method is energy intensive ( $0.6\text{--}1.6 \text{ kWh/m}^3$ )<sup>37</sup> and consumes 36% of the total MBR operating costs.<sup>38</sup> An alternative cost-effective approach for minimizing fouling in anaerobic MBRs is the use of granular activated carbon (GAC) particles to clean the membrane surface by scouring. The energy reported to fluidize the GAC particles in anaerobic fluidized membrane bioreactor (AFMBR) was significantly less ( $0.0107\text{--}0.0580 \text{ kWh/m}^3$ )<sup>18,25</sup> than gas sparging. However, this approach could not be applied in our system as the GAC particles might disrupt the anodic microbial community.

During the complete period of reactor operation, the Ni-HFM membranes were not subjected to any chemical or physical cleaning. The reduced membrane fouling in the

AnEMBR compared to the control reactor could be due to a combination of factors. An appreciable drop in TMP (Figure 3 and SI Figure S2) was observed following increased rates of hydrogen production (Figure 3) when the applied voltage was increased from 0.5 to 0.9 V. SEM images showed a noticeable difference in the biofilm coverage for Ni-HFM operated at 0.5 V (day 62) and following operation at 0.9 V (day 71) (Figure 4). This observation suggests that the increased rate of

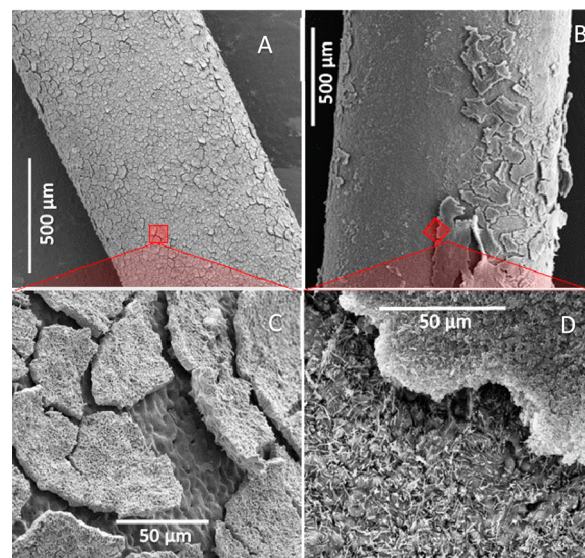


**Figure 4.** Scanning electron micrographs of the Ni-HFM after operation at an applied voltage of 0.5 V (A and C) and 0.9 V (B and D).

hydrogen bubble formation at the electrode surface (SI Figure S3) could provide a means of scouring (self-cleaning) the surface of the membrane. Additionally, the low cathode potential, required to drive the HER,<sup>29</sup> and localized high pH at the cathode electrode surface that results from proton consumption,<sup>29</sup> might have slowed fouling in the AnEMBR system compared to the control reactor. However, further studies are necessary to elucidate the mechanism of fouling in the AnEMBR system and to evaluate the relationship between cathodic physio-chemical reactions and fouling propensity.

**Energy Balance.** The energy content of the biogas produced by the AnEMBR exceeded the electrical energy input to the system to drive  $\text{H}_2$  evolution as well as to recirculate and filter the treated water ( $\eta_E$ ) (Table 2). At an applied voltage of 0.7 V and a volumetric current density of  $11.1 \pm 0.8 \text{ A/m}^3$ , the AnEMBR produced  $3 \text{ mol CH}_4/\text{m}^3$  with a negligible amount of hydrogen in the biogas. Using the higher heating values for methane ( $891 \text{ kJ/mol}$ ), this represents an energy yield of  $2673 \text{ kJ/m}^3$  or  $0.74 \text{ kWh/m}^3$ . However, since the efficiency of converting methane to electricity by combustion processes is only 33%,<sup>25</sup> a maximum of  $0.24 \text{ kWh/m}^3$  of electricity could be generated from the recovered methane. This is sufficient to meet 47% of the electrical energy demand ( $0.51 \text{ kWh/m}^3$ ) at an applied voltage of 0.7 V (Table 2). Although energy neutrality was not achieved under these conditions, the energy required to operate the AnEMBR system ( $0.27 \text{ kWh/m}^3$ ) after subtracting the electrical energy demand ( $0.51 \text{ kWh/m}^3$ ) from the recovered energy ( $0.24 \text{ kWh/m}^3$ ) is still much lower than what is required for large-scale aerobic MBRs ( $1\text{--}2 \text{ kWh/m}^3$ ).

Table 2. Efficiencies and Overall Energy Recoveries of the AnEMBR at Different Applied Voltages

$E_{ap}$	$\eta_E$ (%) <sup>a</sup>	$\eta_S$ (%) <sup>b</sup>	electricity (power supply + pumping) (kWh/m <sup>3</sup> ) <sup>c</sup>	energy recovery (kWh/m <sup>3</sup> ) <sup>d</sup>	net energy (kWh/m <sup>3</sup> )
0.5	158 ± 37	39 ± 2	0.30 ± 0.07	0.46 ± 0.01	0.16 ± 0.07
0.7	146 ± 25	71 ± 11	0.51 ± 0.07	0.74 ± 0.03	0.24 ± 0.1
0.9	105 ± 7	53 ± 6	0.56 ± 0.03	0.58 ± 0.05	0.03 ± 0.04
0.7 <sup>e</sup>	145	71	0.62	0.91	0.29

<sup>a</sup>Energy efficiency relative to the electrical energy input (power supply and pumping). <sup>b</sup>Energy efficiency relative to the added substrate. <sup>c</sup>Based on energy consumption calculations. <sup>d</sup>Based on energy recovery calculations. <sup>e</sup>Operation with 2-Bromoethanesulfonate, a known inhibitor of methanogenesis. Note: Dissolved CH<sub>4</sub> and H<sub>2</sub> were not included in the calculations.

A significant fraction (71%) of the substrate was recovered in the form of biogas (83% CH<sub>4</sub>; <1% H<sub>2</sub>) at 0.7 V (Table 2) and compares favorably with AFMBR technology that can recover 83% of the substrate as methane (both dissolved and gas phases).<sup>25</sup> It should be noted that methane fraction of the biogas (83% at 0.7 V) was appreciably higher than typical percentages for biogas from conventional anaerobic digestion processes (60–75%), in which acetoclastic methanogenesis is the dominant methane production pathway.<sup>39</sup> Acetoclastic methanogenesis produces equal amounts of methane and CO<sub>2</sub>, yielding a biogas with a large proportion of CO<sub>2</sub>.<sup>37</sup> Acetoclastic methanogens were not detected in the AnEMBR system and the relative purity of the biogas was due to essentially complete conversion of the hydrogen gas produced at the cathode to methane by hydrogenotrophic methanogens. In our system the nonmethanogenic step (oxidation of acetate at the anode by exoelectrogens) was physically separated from the methanogenic step which occurred predominantly at the cathode via hydrogenotrophic methanogens (consumption of H<sub>2</sub> and CO<sub>2</sub>). The relative purity of the methane produced in the AnEMBR system is an advantage of producing methane bioelectrochemically. The production of methane by bioelectrochemical methanogenesis will likely not displace biomethane production using anaerobic digesters, especially for high-strength wastewaters.<sup>8</sup> The AnEMBR system will likely be more appropriate for the treatment of relatively dilute wastewaters such as domestic wastewaters.

Addition of 2-bromoethanesulfonate to the reactor at an applied voltage of 0.7 V resulted in a significant increase in hydrogen yields with minimal methane detected in the biogas. Under these conditions and assuming an efficiency limit of a hydrogen fuel cell (based on the higher heating value of hydrogen) of 83% at 25 °C, the energy balance of the AnEMBR was positive (0.14 kWh/m<sup>3</sup>) (Table 2), however, this energy balance would change when using domestic wastewater and scaling up the system.

The largest fraction of electrical energy required by the AnEMBR was for the power supply (>90%) at each applied voltage tested (SI Table S5). Electricity consumption by pumps for recirculation and filtration contributed less than 10% of the overall energy demand (SI Table S5).

**Permeate Water Quality.** The SCOD removal was >95% at all applied voltages tested with permeate SCOD of 0.3 mg/L at 0.7 V, 20 mg/L at 0.5 V, and 10 mg/L at 0.9 V. The TSS in the permeate at the end of a batch cycle was ~17 mg/L. Previous studies integrating MFC with MBR<sup>18,19</sup> reported negligible TSS in the permeate using membranes with pore size of 0.065 μm<sup>19</sup> and 0.1 μm,<sup>18</sup> which are much smaller than the pore size (1 μm) of the Ni-HFM used in this study. Further optimization of the fabrication process can generate hollow fibers with a pore size in the range of ultrafiltration membranes

(2–50 nm) that would yield permeate with improved water quality.<sup>19</sup>

**Outlook.** The developed AnEMBR system represents a truly integrated proof-of-concept hybrid MEC-MBR system that incorporated a conductive, Ni-HFM cathode within a MEC. Our proof-of-concept AnEMBR was effective in the treatment of low-organic strength solutions in terms of SCOD. The system was operated for 70 days without replacement or cleaning (e.g., backwashing or chemical treatment) of the membrane and observations suggest that biofouling could be mitigated by increasing rates of biogas production which can be controlled by regulating the applied voltage. However, further studies are necessary to evaluate the relationship between biogas (H<sub>2</sub> and CH<sub>4</sub>) production rate and biofouling.

The AnEMBR system recovered 71% of the substrate energy as methane rich biogas (83% CH<sub>4</sub>; < 1% H<sub>2</sub>) at an applied voltage of 0.7 V. The dissolved methane was not measured in this study, but our calculations show that this would be <6% of the total methane generated (detailed information in the SI) at an applied voltage of 0.7 V (SI Figure S4). Dissolved methane needs to be considered in future AnEMBR applications because it is a risk in terms of greenhouse effect if it is released in the effluent<sup>40</sup> and it is considered as an additional energy that could be recovered using available commercial systems such as gas permeable membranes and air stripping, but the economic feasibility of these systems has not yet been fully evaluated.<sup>40,41</sup>

The energy required to operate the AnEMBR was significantly lower than what is needed for aerobic MBRs. It should be noted that the process design and operation were not optimized in this study for energy considerations. For example, the spacing between the electrodes was 2 cm and the specific cathode surface area was 4 m<sup>2</sup>/m<sup>3</sup>. By implementing improvements to reactor design and operation such as increasing the specific cathode surface area<sup>21</sup> and reducing the electrode spacing to minimize ohmic losses,<sup>21</sup> it should be possible to improve the recovery of energy as biogas from low strength wastewaters using the AnEMBR technology and to achieve an energy-neutral process. Also, improved reactor design will allow for higher currents at lower applied voltages, which would reduce treatment time. However, the robustness of the system in terms of treatment performance and energetics should be evaluated in the future with real domestic wastewater and under continuous mode of operation.

## ■ ASSOCIATED CONTENT

### ● Supporting Information

Theoretical and measured hydrogen and methane production rates, TMP measurements, photographs of nickel hollow-fiber membrane cathodes showing bubble formation, electron balance, DNA extraction and qPCR analysis, additional experiments with duplicate AnEMBR to determine level of reproducibility in performance, comparison of hydrogen



production rates, cost of materials to fabricate conductive porous Ni-HFM, and breakdown of electrical energy required for the power supply, pumping for recirculation and filtration. This material is available free of charge via the Internet at <http://pubs.acs.org>.

## AUTHOR INFORMATION

### Corresponding Author

\*Phone: +966-5-44700129; e-mail: [pascal.saikaly@kaust.edu.sa](mailto:pascal.saikaly@kaust.edu.sa).

### Author Contributions

<sup>†</sup>K.P.K and C.M.W. contributed equally to this work

### Notes

The authors declare no competing financial interest.

## ACKNOWLEDGMENTS

This work was supported by a SABIC Fellowship (K.K.) as well as a PhD fellowship award (C.W.) and discretionary investigator funds (P.S.) from the King Abdullah University of Science and Technology (KAUST).

## REFERENCES

- (1) Olsson, G. *Water and Energy: Threats and Opportunities*; IWA Publishing, 2012.
- (2) McCarty, P. L.; Bae, J.; Kim, J. Domestic wastewater treatment as a net energy producer—Can this be achieved? *Environ. Sci. Technol.* **2011**, *45* (17), 7100–7106.
- (3) Heidrich, E. S.; Curtis, T. P.; Dolfing, J. Determination of the internal chemical energy of wastewater. *Environ. Sci. Technol.* **2011**, *45* (2), 827–832.
- (4) Liu, H.; Grot, S.; Logan, B. E. Electrochemically assisted microbial production of hydrogen from acetate. *Environ. Sci. Technol.* **2005**, *39* (11), 4317–4320.
- (5) Rozendal, R. A.; Hamelers, H. V. M.; Euverink, G. J. W.; Metz, S. J.; Buisman, C. J. N. Principle and perspectives of hydrogen production through biocatalyzed electrolysis. *Int. J. Hydrogen Energy* **2006**, *31* (12), 1632–1640.
- (6) Call, D.; Logan, B. E. Hydrogen production in a single chamber microbial electrolysis cell lacking a membrane. *Environ. Sci. Technol.* **2008**, *42* (9), 3401–3406.
- (7) Ge, Z.; Li, J.; Xiao, L.; Tong, Y.; He, Z. Recovery of electrical energy in microbial fuel cells. *Environ. Sci. Technol. Lett.* **2013**, *1*, 137–141.
- (8) Luo, X.; Zhang, F.; Liu, J.; Zhang, X.; Huang, X.; Logan, B. E. Methane production in microbial reverse-electrodialysis methanogenesis cells (MRMCs) using thermolytic solutions. *Environ. Sci. Technol.* **2014**, *48* (15), 8911–8918.
- (9) Heidrich, E. S.; Dolfing, J.; Scott, K.; Edwards, S. R.; Jones, C.; Curtis, T. P. Production of hydrogen from domestic wastewater in a pilot-scale microbial electrolysis cell. *Appl. Microbiol. Biotechnol.* **2013**, *97* (15), 6979–6989.
- (10) Lu, L.; Ren, N.; Zhao, X.; Wang, H.; Xing, D. Hydrogen production, methanogen inhibition and microbial community structures in psychrophilic single-chamber microbial electrolysis cells. *Energy Environ. Sci.* **2011**, *4*, 1329–1336.
- (11) Wang, Y.-K.; Sheng, G.-P.; Shi, B.-J.; Li, W.-W.; Yu, H.-Q. A novel electrochemical membrane bioreactor as a potential net energy producer for sustainable wastewater treatment. *Sci. Rep.* **2013**, *3* (1864), 1–6.
- (12) Wang, Y.-P.; Liu, X.-W.; Li, W.-W.; Li, F.; Wang, Y.-K.; Sheng, G.-P.; Zeng, R. J.; Yu, H.-Q. A microbial fuel cell—membrane bioreactor integrated system for cost-effective wastewater treatment. *Appl. Energy* **2012**, *98*, 230–235.
- (13) Liu, J.; Liu, L.; Gao, B.; Yang, F. Integration of bio-electrochemical cell in membrane bioreactor for membrane cathode fouling reduction through electricity generation. *J. Membr. Sci.* **2013**, *430*, 196–202.
- (14) Wang, Y.-K.; Sheng, G.-P.; Li, W.-W.; Huang, Y.-X.; Yu, Y.-Y.; Zeng, R. J.; Yu, H.-Q. Development of a novel bioelectrochemical membrane reactor for wastewater treatment. *Environ. Sci. Technol.* **2011**, *45* (21), 9256–9261.
- (15) Ge, Z.; Ping, Q.; He, Z. Hollow-fiber membrane bioelectrochemical reactor for domestic wastewater treatment. *J. Chem. Technol. Biotechnol.* **2013**, *88* (8), 1584–1590.
- (16) Li, J.; Ge, Z.; He, Z. Advancing membrane bioelectrochemical reactor (MBER) with hollow-fiber membranes installed in the cathode compartment. *J. Chem. Technol. Biotechnol.* **2013**, DOI: 10.1002/jctb.4206.
- (17) Tian, Y.; Ji, C.; Wang, K.; Le-Clech, P. Assessment of an anaerobic membrane bio-electrochemical reactor (AnMBER) for wastewater treatment and energy recovery. *J. Membr. Sci.* **2014**, *450*, 242–248.
- (18) Ren, L.; Ahn, Y.; Logan, B. E. A two-stage microbial fuel cell and anaerobic fluidized bed membrane bioreactor (MFC-AFMBR) system for effective domestic wastewater treatment. *Environ. Sci. Technol.* **2014**, *48* (7), 4199–4206.
- (19) Malaeb, L.; Katuri, K. P.; Logan, B. E.; Maab, H.; Nunes, S. P.; Saikaly, P. E. A hybrid microbial fuel cell membrane bioreactor with a conductive ultrafiltration membrane biocathode for wastewater treatment. *Environ. Sci. Technol.* **2013**, *47* (20), 11821–11828.
- (20) Hanson, C. California brewery toasts new biogas system opening. In *Biomass Magazine*, 11 March 2014 <http://biomassmagazine.com/articles/10108/california-brewery-toasts-new-biogas-system-opening/>.
- (21) Sleutels, T. H. J. A.; Ter Heijne, A.; Buisman, C. J. N.; Hamelers, H. V. M. Bioelectrochemical systems: An outlook for practical applications. *ChemSusChem* **2012**, *5* (6), 1012–1019.
- (22) Meng, B.; Tan, X.; Meng, X.; Qiao, S.; Liu, S. Porous and dense Ni hollow fibre membranes. *J. Alloys Compd.* **2009**, *470* (1), 461–464.
- (23) Cheng, S.; Xing, D.; Call, D. F.; Logan, B. E. Direct biological conversion of electrons into methane by electromethanogenesis. *Environ. Sci. Technol.* **2009**, *43* (10), 3953–3958.
- (24) Cusick, R. D.; Bryan, B.; Parker, D. S.; Merrill, M. D.; Mehanna, M.; Kiely, P. D.; Liu, G.; Logan, B. E. Performance of a pilot-scale continuous flow microbial electrolysis cell fed winery wastewater. *Appl. Microbiol. Biotechnol.* **2011**, *89* (6), 2053–2063.
- (25) Kim, J.; Kim, K.; Ye, H.; Lee, E.; Shin, C.; McCarty, P. L.; Bae, J. Anaerobic fluidized bed membrane bioreactor for wastewater treatment. *Environ. Sci. Technol.* **2011**, *45* (2), 576–581.
- (26) APHA. *Standard Methods for the Examination of Water and Wastewater*, 20th ed.; American Public Health Association, American Water Works Association, Water Environment Federation: Washington DC, 1998.
- (27) Clauwaert, P.; Verstraete, W. Methanogenesis in membraneless microbial electrolysis cells. *Appl. Microbiol. Biotechnol.* **2009**, *82*, 829–836.
- (28) Rader, G. K.; Logan, B. E. Multi-electrode continuous flow microbial electrolysis cell for biogas production from acetate. *Int. J. Hydrogen Energy* **2010**, *35* (17), 8848–8854.
- (29) Logan, B. E.; Call, D.; Cheng, S.; Hamelers, H. V. M.; Sleutels, T. H. J. A.; Jeremiasse, A. W.; Rozendal, R. A. Microbial electrolysis cells for high yield hydrogen gas production from organic matter. *Environ. Sci. Technol.* **2008**, *42* (23), 8630–8640.
- (30) Garcia, J.-L.; Patel, B. K.; Ollivier, B. Taxonomic, phylogenetic, and ecological diversity of methanogenic archaea. *Anaerobe* **2000**, *6* (4), 205–226.
- (31) Jeremiasse, A. W.; Hamelers, H. V. M.; Saakes, M.; Buisman, C. J. N. Ni foam cathode enables high volumetric H<sub>2</sub> production in a microbial electrolysis cell. *Int. J. Hydrogen Energy* **2010**, *35* (23), 12716–12723.
- (32) Selembo, P. A.; Merrill, M. D.; Logan, B. E. The use of stainless steel and nickel alloys as low-cost cathodes in microbial electrolysis cells. *J. Power Sources* **2009**, *190* (2), 271–278.
- (33) Selembo, P. A.; Merrill, M. D.; Logan, B. E. Hydrogen production with nickel powder cathode catalysts in microbial electrolysis cells. *Int. J. Hydrogen Energy* **2010**, *35* (2), 428–437.



- (34) Miles, M. H. Evaluation of electrocatalysts for water electrolysis in alkaline solutions. *J. Electroanal. Chem.* **1975**, *60* (1), 89–96.
- (35) Cheng, S.; Liu, H.; Logan, B. E. Power densities using different cathode catalysts (Pt and CoTMPP) and polymer binders (Nafion and PTFE) in single chamber microbial fuel cells. *Environ. Sci. Technol.* **2006**, *40*, 364–369.
- (36) Siegert, M.; Yates, M. D.; Call, D. F.; Zhu, X.; Spormann, A.; Logan, B. E. Comparison of nonprecious metal cathode materials for methane production by electromethanogenesis. *ACS Sus. Chem. Eng.* **2014**, *2* (4), 910–917.
- (37) Martin, I.; Pidou, M.; Soares, A.; Judd, S.; Jefferson, B. Modeling the energy demands of aerobic and anaerobic membrane bioreactors for wastewater treatment. *Environ. Technol.* **2011**, *32* (9), 921–932.
- (38) Verricht, B.; Maere, T.; Nopens, I.; Brepols, C.; Judd, S. The cost of large-scale hollow fibre MBR. *Water. Res.* **2010**, *44* (18), 5274–5283.
- (39) Parkin, G. F.; Owen, W. F. Fundamentals of anaerobic digestion of wastewater sludges. *J. Environ. Eng.* **1986**, *112* (5), 867–920.
- (40) Liu, Z.-h.; Yin, H.; Dang, Z.; Liu, Y. Dissolved methane: A hurdle for anaerobic treatment of municipal wastewater. *Environ. Sci. Technol.* **2013**, *48* (2), 889–890.
- (41) Yoo, R.; Kim, J.; McCarty, P. L.; Bae, J. Anaerobic treatment of municipal wastewater with a staged anaerobic fluidized membrane bioreactor (SAF-MBR) system. *Bioresour. Technol.* **2012**, *120*, 133–139.
- (42) Werner, C. M.; Logan, B. E.; Saikaly, P. E.; Amy, G. L. Wastewater treatment, energy recovery and indirect desalination using an air-cathode osmotic microbial fuel cell. *J. Membr. Sci.* **2013**, *428*, 116–122.